Biomed Eng Lett (2014) 4:396-402
DOI 10.1007/s13534-014-0159-6

ORIGINAL ARTICLE

Mechanical Eye Model for Evaluating Intraocular Pressure Measurements

Kutaiba Saleh, Volkmar Unger, Alexander Dietzel, Detlef Heydenreich, Rico Großjohann, Clemens Jürgens, Frank Tost and Jens Haueisen

Received: 23 July 2014 / Revised: 22 October 2014 / Accepted: 28 October 2014

Abstract
Purpose For the development of new intraocular pressure (IOP) measurement devices, as well as for comparison with existing devices it is important to consider the various biomechanical properties of the eye in test setups. Therefore, a controllable physical phantom with flexibility in the adjustment of biomechanical parameters and geometries is being proposed and analyzed.
Methods Different configurations of a mechanical eye model are simulated together with the applanation process, based on the finite element method (FEM). Forming tools are designed to produce artificial corneas with variable thicknesses and stiffness's using injection molding. An apparatus is assembled for controlling and evaluating the phantom eye in connection with a piezoelectric IOP test sensor. Measurements are also performed using the commercially available non-contact tonometer NCT-800.
Results Simulation results for surface pressure and stress distribution at the cornea together with the pressure in the central part of the applanation body show that the pressure reaches a maximum when the local stress is centrally concentrated and decreases to a stable level afterwards. More rigid corneas result in higher maximum values for the pressure. The measurements with the piezoelectric IOP test sensor are in good agreement with the simulation results. The NCT-800 measurements show a significant influence of the biomechanical properties of the cornea on measured IOPs.
Conclusion Our phantom is suitable for describing the effect of biomechanical characteristics of the human eye on tonometric measurements and will facilitate the evaluation of new tonometry systems.

Keywords IOP, Eye model, Intraocular pressure, Biomechanical properties

Kutaiba Saleh, Volkmar Unger, Alexander Dietzel (✉), Jens Haueisen
Institute of Biomedical Engineering and Informatics, Ilmenau University of Technology, D-98684 Ilmenau, Germany
Tel : +493677691957 / Fax : +493677691311
E-mail : alexander.dietzel@tu-ilmenau.de

Detlef Heydenreich
Elektronik & Präzisionsbau Saalfeld (EPSa) GmbH, D-07745 Jena, Germany

Rico Großjohann, Clemens Jürgens, Frank Tost
Department of Ophthalmology, Ernst-Moritz-Arndt University of Greifswald, D-17475 Greifswald, Germany

INTRODUCTION

Numerous clinical studies have been conducted to evaluate the accuracy of intraocular pressure (IOP) measurements on the human eye and to compare IOP results obtained by different tonometry devices [1]. Studies show that measured IOPs are influenced by the dimensions and the rigidity of the cornea and by other biomechanical properties of the eye [2, 3]. For example, changes in corneal thickness and curvature induced by laser photorefractive procedures significantly affect the estimation of IOPs [4-6]. For the development of new IOP measurement devices, as well as for the cross comparison of and with existing IOP measurement devices it is therefore important to consider these mechanical properties in test setups. Physical phantoms are suitable for testing and comparing new IOP measurement devices due to their flexibility in the adjustment of the mechanical properties of the eye and due to fact that these phantoms can be well controlled. Thus, there is a need to develop a model of the human eyeball that accurately describes the broad variation in the biomechanical properties and geometries of the eye [7, 8].

Computer models, typically based on the finite element method (FEM), incorporate various geometric parameters and material properties of the eye [9]; these models also provide the basis for the development of mechanical (physical)

eye models, which can then be used to empirically analyze tonometry systems. The influence of different known biomechanical characteristics on measured IOPs can be tested using such a mechanical eye model. To adequately incorporate a variety of biomechanical characteristics, as well as eye diseases (e.g., Keratoconus) and even surgical results [8], the model should consist of exchangeable components. Thus, we developed a mechanical eye model (BiomechEye) with exchangeable corneas and sclera. We exemplify the possible changes of biomechanical properties in BiomechEye by experiments with different central corneal thicknesses (CCTs) and different Young's moduli. BiomechEye is controlled by several control circuits to simulate the dynamic behavior of the eye and to evaluate corresponding inner pressures.

MATERIAL AND METHODS

Numerical design for the mechanical eye

FEM simulations were performed with ANSYS (ANSYS Inc., Canonsburg, PA, USA) to test different configurations of a mechanical eye model and to simulate the applanation process. The applied mechanical properties (geometrics and materials) of the FEM models are primary based on the works of Al-Sukhun *et al.* (2011) [10], Bocskai *et al.* (2013) [11], Cabrera Fernández *et al.* (2005) [7], Crouch *et al.* (2005) [12], Kling *et al.* (2013) [13], Nejad *et al.* (2014) [14], Power *et al.* (2001) [15], Rossi *et al.* (2012) [16], Roy *et al.* (2011) [9], Srodka (2011) [17], Studer *et al.* (2010) [18] and Uchio *et al.* (1999) [19].

There were two main goals regarding the simulations for the different configurations of the model eye. First of all to obtain a force transmissions across the model eye yielding model stability in terms of exchangeability of parts and then an optimal design for the intersection of sclera and cornea, which can significantly influence IOP measurements [20].

The FEM model was constructed based on general anatomical information [21], with sizes and shapes resembling a normal human eye (Fig. 1 - a1). The mechanical eye model consisted of three flexible parts: cornea, sclera front and sclera rear. All were meshed using SOLID187 elements and solved under steady state conditions. The material properties used for silicon were isotropic elastic with Young's modulus of 1 MPa and a Poisson ratio of 0.49. In total, 43,532 nodes and 24,686 elements were used for the complete eye model with bonded contact defined as contact type between the model parts. A static analysis with large deformations, nonlinear geometric effects and full Newton-Raphson options was performed. The FEM solution for the connection between cornea and sclera features a form-fitted self-centering interleaving area (Figs. 1 - a1 and 1 - a2). This configuration assures smooth force transmission and uniformly distributed stresses in the cornea.

Another FEM model was constructed to simulate the applanation process. The aim was to get detailed information about the surface pressure and stress distribution of the cornea for different indentation depths at the applanation area. Therefore, a flexible cornea with a fixed position and static pressure of 2666 Pa inside and a movable cylinder with diameter of 3.06 mm were modeled. Both were meshed using SOLID187 and SOLID186 elements and solved under steady state conditions. The material properties for the cornea (silicon) were the same like mentioned above but Young's modulus was also simulated for 0.2 MPa and 0.5 MPa. The properties for the cylinder (structural steel) were isotropic elastic with Young's modulus of 200,000 MPa and a Poisson ratio of 0.3. In total, 78,048 nodes and 29,410 elements were used with frictional contact (coefficient 0.1) defined as contact type between the cornea and the cylinder. A static analysis was performed using large deformations, a preconditioned conjugate gradient solver, and nonlinear geometric effects.

Development of the mechanical eye

Forming tools were designed to allow the production of artificial corneas with variable thicknesses and stiffness's using injection molding. The stiffness was regulated by the mechanical properties of the material whereas the thickness was adjusted by the forming tool. Tissue injuries such as scarves or abnormal cornea bowings can be integrated into the shape. The forming tools (Fig. 1b, left) were designed to construct corneas with variable inner and outer radii; it consists of an exchangeable and adjustable core (Fig. 1b, a) which determines the inner radius of the cornea, and a counterpart (Fig. 1b, b) which determines the outer radius. The position of the core is adjusted by a fine-threaded screw which determines the cornea thickness. In the case of a concentrically adjusted core, the cornea thickness is constant throughout, determined by the difference between the inner and outer radii. A proximal displacement of the core relative to its counterpart creates a thickness gradient in which the cornea thickness increases from the center to the periphery. The cornea thickness can be varied from 0.1 to 1 mm in increments of 0.05 mm. The sclera components were formed by non-adjustable forming tools (Fig. 1b, middle and right) as the influence of sclera thickness on stiffness is not considered here; however, the stiffness can be varied by using materials with different Young's moduli. The mechanical properties of the materials (linear elastic representation) used in the model were chosen to be similar to those observed in the human cornea and sclera [20, 22-23]. The raw material used for the model components was silicone (Wacker, Munich, Germany). Forming of models was accomplished in

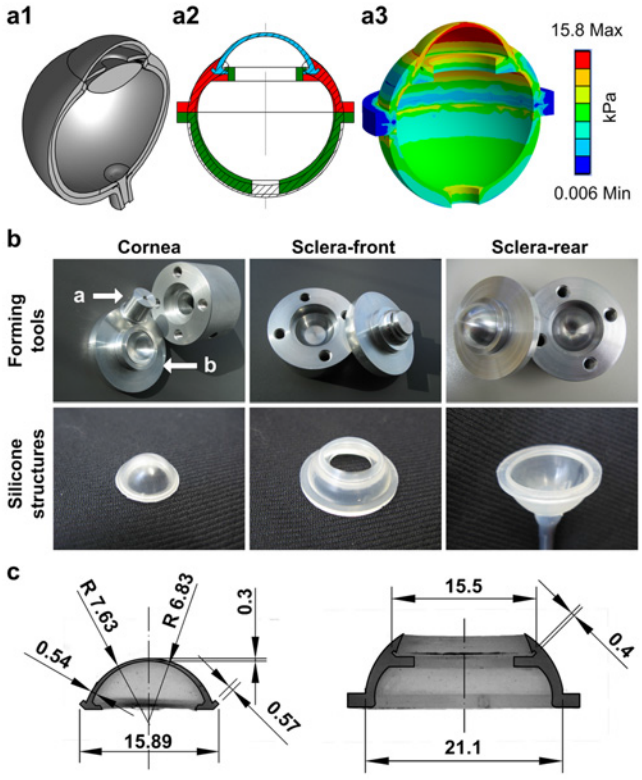

Fig. 1. (a1) Schematic of a human eye. (a2) Construction of a mechanical eye model with exchangeable parts (colored), overlain by the configuration of a biological eye (hatched). (a3) Mechanical stress distribution determined by a FEM simulation. (b) Forming tools and resulting silicone eye structures. Left: Cornea; middle: front part of the sclera; right: rear part of the sclera with connecting tube. The forming tool for the cornea consisted of an adjustable core (b-a) and a counterpart (b-b). (c) Photographs and overlain schematics (black lines) of the produced cornea (left) and the front part of the sclera (right) and their dimensions measured after production in cross-sectional views (in mm).

15 min at a temperature of 175°C.

Cross sections of control samples of a cornea and of the front part of the sclera were measured as shown in Fig. 1c; in the example, the CCT is 0.3 mm and the peripheral thickness is 0.54 mm. The thickness distribution of the cornea is equivalent to typical human parameters, as defined by the radii of curvature of the cornea on inner and outer surfaces. The difference between the diameter of the cornea and that of the sclera fitting is caused by manufacturing tolerances. To assure a smooth force transmission, uniformly distributed stress, and a leak proof connection between cornea and sclera, mechanical interlocking and clamping structures were realized (Fig. 1).

Assembly of the mechanical eye

Fig. 2 shows the apparatus for evaluating the BiomechEye. To assemble the BiomechEye, the cornea was clipped into the front part of the sclera (Fig. 1). The front and rear parts of the sclera were joined by a flute between two aluminum coils which were laterally anchored to stabilize their positions. The BiomechEye was connected to a reservoir of an incompressible transmission medium (water was used in the tests). Air bubbles were vented from the BiomechEye by turning the bonded tube connection upwards. A valve was opened for both filling and venting, and closed while measuring IOPs. An adjustable flow valve can be used to emulate the natural outflow of aqueous humor.

The BiomechEye was filled with water to adjust the inner pressure. The pressure actuator was a stepping motor with a screw gear and a piston, used in conjunction with the pressure tube. Possible pressure values ranged from 0 to 100 mmHg in increments of 0.1 mmHg. Pressure was measured

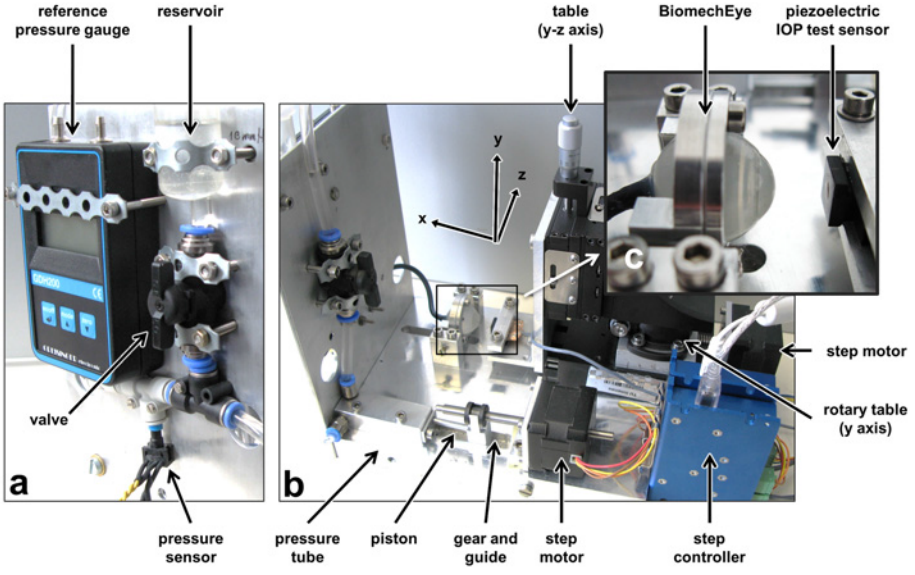

Fig. 2. Apparatus for evaluating the eye model: (a) rear view; (b) lateral view; (c) inset shows BiomechEye and the piezoelectric IOP test sensor.

by a gauge mounted at the height of the BiomechEye, calibrated using a fine manometer. A stepping controller steered the stepping motor, which moved the piezoelectric IOP test sensor against the eye. The driving direction was manipulated by a linear table and a rotary table.

Control circuits

The control circuit for establishing the pressure in the BiomechEye is represented in Fig. 3 (top portion). The output voltage of the pressure gauge was recorded by an I/O device (DAQ card). Linear voltage characteristics were scaled to pressure and the offset was eliminated. LabView (National Instruments, Inc., Austin, TX, USA) software provided the nominal pressure, monitored the actual pressure, and gave a directional signal to the stepping controller representing the difference between the actual and the nominal pressure in the BiomechEye. The control circuit of the IOP test sensor (Fig. 3, bottom portion) can be replaced by any tonometry system. Velocities and displacements were transmitted to the controller of the stepping motor using a LabView interface, which was responsible for moving the IOP test sensor. The output voltage of the IOP test sensor was recorded by the I/O device and stored in an output file, together with the inner pressure in the BiomechEye.

Piezoelectric IOP test sensor

A force sensor (Mirow Systemtechnik GmbH, Berlin, Germany) was used to evaluate the influence of biomechanical characteristics of the BiomechEye on IOP. The force sensor has a round effective measurement area with a diameter of 0.8 mm. It is mounted centrally on a 10 × 10 mm plate (Fig. 2, piezoelectric IOP test sensor). When the sensor is placed against the cornea, the sensor signal corresponds to the force on the sensor surface under the condition that the applanation area exceeds the effective sensor measurement area. During the experiments, the sensor was centrally positions against the cornea.

Non-contact tonometer

Measurements were performed using a commercially available non-contact tonometer (NCT-800, Rodenstock, WECO Optik GmbH, Düsseldorf, Germany). The inner pressure of the BiomechEye was varied from 10 to 30 mmHg in increments of 5 mmHg. The Young's moduli of corneas ranged from 0.6 to 7 MPa and CCTs were from 0.1 to 0.5 mm. All measurements were repeated five times. The sclera and supporting parts were covered to avoid reflections, which influence the self-positioning system of the tonometer.

RESULTS

The simulated surface pressures and stress distributions of the cornea for two indentation depths at the applanation area are shown in Fig. 4 (top). When the contact area is relatively small (Fig. 4, top, State 1), the surface pressure is much higher than it is in cases where the applanation area is large

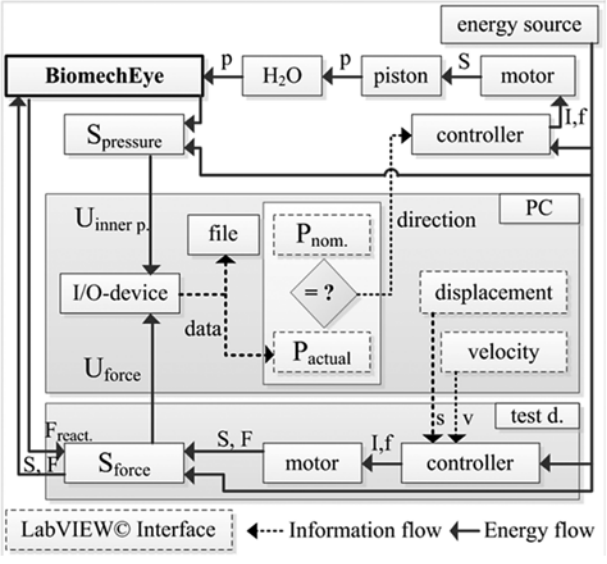

Fig. 3. Components and circuits controlling the eye model experiments, including the BiomechEye and the piezoelectric IOP test sensor. I: current; F: force; f: frequency; p: pressure; s: displacement; v: velocity.

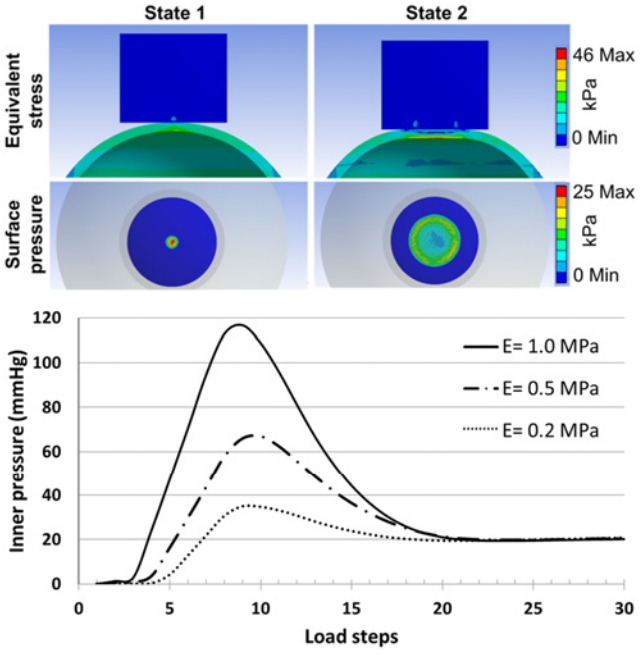

Fig. 4. Surface pressures corresponding to load step 9 (state 1, left) and 20 (state 2, right) with Young's modulus of 1 MPa. Bottom: pressure in the central part of the cylinder during the applanation process for different Young's moduli.

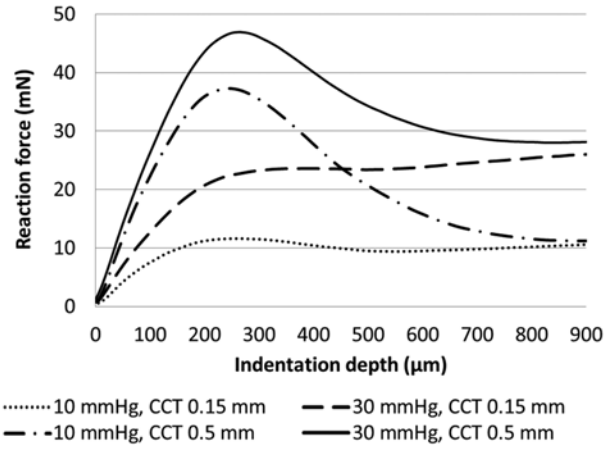

Fig. 5. The reaction force as a function of indentation depth for inner cornea pressures of 10 and 30 mmHg and CCTs of 0.15 and 0.5 mm. The Young's modulus of the cornea was 1 MPa.

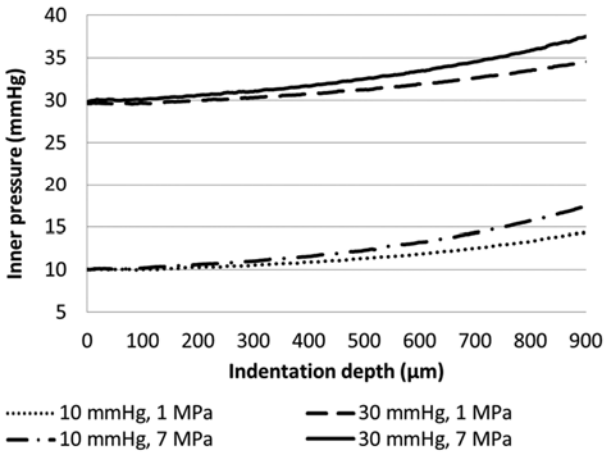

Fig. 6. Change of the inner pressure during applanation of the cornea of the BiomechEye using sclera with Young's moduli of 1 and 7 MPa, for starting inner pressures of 10 and 30 mmHg.

(Fig. 4, top, State 2). This behavior is caused by the interaction of a directional force on a spherical fluid-filled body, as constrained by the sphere's inherent rigidity. The planar applanation area causes a stress distribution on the cornea with local stress concentrations on the periphery (Fig. 4, top, State 2). The calculated pressure curves on the central part of the cylinder confirm this effect Fig. 4 (bottom). The pressure at the center reaches a maximum when the local stress is centrally concentrated (State 1, load step 9). With increasing load steps, the pressure at the center decreases until it reaches a stable level (State 2, load step 20). The maximum value dependents on the Young's modulus which defines the rigidity of the material. A more rigid cornea results in a higher maximum value for the calculated pressure.

Fig. 5 shows examples of piezoelectric IOP test sensor recordings. The force detected by the sensor increases after the initial contact of the sensor with the cornea, reaching a local maximum at about 300 μm. At greater indentations, the force value typically decreases to a relatively stable level. The difference between the maximum force and the ensuing stable level can be used to define a parameter of rigidity of the cornea. At greater indentations, the value of the force (the stabilized level) directly corresponds to the inner pressure in the BiomechEye. The relationship between the force sensor measurements and the indentation depth on the BiomechEye is in good agreement with the simulation results.

In another application of BiomechEye, we investigated changes in intraocular pressure resulting from volume

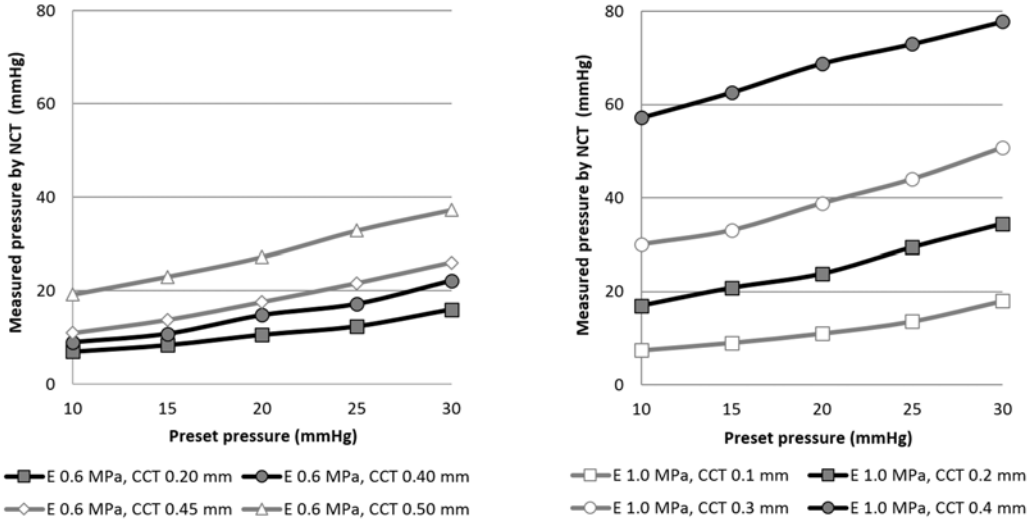

Fig. 7. Per NCT-800 measured pressures as a function of preset pressure values in the BiomechEye, for a range of CCTs from 0.1 mm to 0.5 mm and Young's moduli of 0.6 MPa (left) and 1 MPa (right). Graphs in black have the same CCT at different Youngs moduli.

deformation due to applanation [24]. Our results show that the increase in inner pressure during the measuring process can significantly influence the measurements. The increase in inner pressure depends on the elasticity of the sclera and the indentation depth, as shown in Fig. 6. By simultaneously recording the actual inner pressures and the tonometric measurements, using BiomechEyes with different biomechanical properties, correlations between initial and final inner pressures are revealed. These correlations are the basis for calculations of the IOP derived from tonometric measurements of the eye, and of the dependence of the IOP on the mechanical properties of particular eye structures and configurations.

Results of the tonometer measurements show a significant influence of the biomechanical properties of the cornea on measured IOPs. The relationship between preset and measured pressures for different CCTs and Young's moduli are shown in Fig. 7. Data values represent the average of five measurements; relative standard deviations did not exceed 2.1 mmHg.

Each curve in Fig. 7 shows a nearly linear relationship. Increasing preset pressure values in the BiomechEye lead to increasing pressure values measured by NCT. The curves show different offsets and slopes. Both depend on CCT and Young's modulus. Artificial corneas with increasing CCT result in curves with increasing offset and slope. Offset and slope increase even more in the set of curves with higher Young's modulus (Fig. 7. right).

DISCUSSION

Our results demonstrate that the BiomechEye is suitable for describing the effect of biomechanical characteristics of the human eye on tonometric measurements. Using the closed loop circuit, the pressure can be adjusted to emulate pressure fluctuations, such as those caused by the human pulse. With the help of other forming tools and resulting silicone eye structures our setup can be used to develop models with biomechanical characteristics of e.g. aging or surgically altered eyes. Such a setup can be used to evaluate and compare IOP measurement devices.

Furthermore, we found that small variations in the biomechanical parameters can influence the measurements of the non-contact tonometer. Recordings from the NCT-800 tonometer were used to select the artificial corneas in which the values measured by the tonometer were close to the nominal IOPs. The selection of corneas depends on the measurement principle of the tonometry device in use, because the biomechanical parameters of the cornea have different effects on the recording instrument. The NCT is known to have some difficulties in the repeatability of measurements (repeatability coefficient 3.2 mmHg), mainly because the measurement can be done on different times during the ocular pulse amplitude which effects the IOP [26, 27].

Even though the conditions for temperature and illumination were kept constant, not all artificial corneas could be successfully measured with the NCT-800. Only the CCT values 0.2 mm and 0.4 mm are part of the set of curves for both Young's moduli (Fig. 7). The basic measurement principle of the NCT-800 causes problems when measuring artificial silicone corneas. In the NCT-800, a nozzle is moved to the central corneal positions by maximizing the reflexivity signal, a compressed air pulse deforms the cornea and the resulting deformation is measured by means of IR radiation. Our silicone corneas have a lower reflexivity compared to human eyes. To improve the reflexivity of the artificial corneas they were wiped with a cotton wool flannel saturated with oil (low viscosity) to cover them with a thin film of oil. The oily surface enhanced the reflexivity, which subsequently enabled the successful measurements for most artificial corneas (curves in Fig. 7 were only plotted if all five repeated measurements were successful). Nevertheless, variations in the measurement values can partly be explained by slightly different measurement positions caused by inhomogeneous oil moistening and by the limited repeatability of the NCT in general.

The impact of CCT on the IOP measurement was investigated by non-contact tonometry on 437 subjects [25]. The authors found a positive correlation between CCT and IOP, suggesting that CCT is an important parameter for the interpretation of IOP measurements. Our results are in good agreement with this conclusion.

Both the cornea and the sclera are known to be hyperelastic and anisotropic [28, 29]. In our model we used so far only elastic and isotropic materials, which limits the results presented above. For example, at high pressure levels a nonlinear response would imply a different rigidity of the eye that would differently influence its response to the indentation test and to the flattening of the NCT-800. However, our setup principally allows for the use of hyperelastic and anisotropic materials in future studies.

The BiomechEye setup is also suitable for experiments with enucleated eyes (e.g. pig). Therefore, a special mounting unit was designed to fixate the eye and to provide two separate access ports to regulate the inner eye pressure. The ports can be used in connection with cannulas to gain access either to the anterior or posterior chamber and the vitreous body. Pilot tests with this equipment were successfully carried out on freshly excised pig eyes.

Future work will include an investigation of characteristics such as temperature and humidity, which are important environmental conditions that can affect pressure measurements, and which can be adjusted and controlled by a control

circuit. In addition, a new design for adjustable forming tools will allow for variations in sclera thickness, and thus the investigation of the influence of sclera geometry on IOPs.

ACKNOWLEDGEMENTS

The authors gratefully acknowledge the financial support of the Thüringer Aufbaubank (TAB: 2009VF0025) and BMBF (3IPT605X, 3IPT605A).

CONFLICT OF INTEREST STATEMENTS

Saleh K declares that he has no conflict of interest in relation to the work in this article. Unger V declares that he has no conflict of interest in relation to the work in this article. Dietzel A declares that he has no conflict of interest in relation to the work in this article. Heydenreich D declares that he has no conflict of interest in relation to the work in this article. Großjohann R declares that he has no conflict of interest in relation to the work in this article. Jürgens C declares that he has no conflict of interest in relation to the work in this article. Tost F declares that he has no conflict of interest in relation to the work in this article. Haueisen J declares that he has no conflict of interest in relation to the work in this article.

REFERENCES

[1] Lamparter J, Hoffmann EM. Measuring intraocular pressure by different methods. Ophthalmologe. 2009; 106(8):676-82.
[2] Kwon TH, Ghaboussi J, Pecknold DA, Hashash YMA. Effect of cornea material stiffness on measured intraocular pressure. J Biomech. 2008; 41(8):1707-13.
[3] Harada Y, Hirose N, Kubota T, Tawara A. The influence of central corneal thickness and corneal curvature radius on the intraocular pressure as measured by different tonometers: noncontact and goldmann applanation tonometers. J Glaucoma. 2008; 17(8):619-25.
[4] Hsu SY, Chang MS, Lee CJ. Intraocular pressure assessment in both eyes of the same patient after laser in situ keratomileusis. J Cataract Refract Surg. 2009; 35(1):76-82.
[5] Kirwan C, O'Keefe M. Measurement of intraocular pressure in LASIK and LASEK patients using the Reichert Ocular Response Analyzer and Goldmann applanation tonometry. J Refract Surg. 2008; 24(4):366-70.
[6] Qazi MA, Sanderson JP, Mahmoud AM, Yoon EY, Roberts CJ, Pepose JS. Postoperative changes in intraocular pressure and corneal biomechanical metrics Laser in situ keratomileusis versus laser-assisted subepithelial keratectomy. J Cataract Refract Surg. 2009; 35(10):1774-88.
[7] Cabrera Fernández D, Niazy AM, Kurtz RM, Djotyan GP, Juhasz T. Finite element analysis applied to cornea reshaping. J Biomed Opt. 2005; doi:10.1117/1.2136149.
[8] Hien M, Yang THJ, Reuben RL, Else RW. Dynamic measurement of intraocular pressure using a mechanical model of the human eye. Stud Health Technol Inform. 2008; 133:112-22.
[9] Roy AS, Dupps WJ. Patient-specific modeling of corneal refractive surgery outcomes and inverse estimation of elastic property changes. J Biomech Eng. 2011; doi: 10.1115/1.4002934.
[10] Al-Sukhun J, Penttilä H, Ashammakhi N. Orbital Stress Analysis: Part II: Design and Fixation of Autogenous Bone Graft Used to Repair Orbital Blowout Fracture. J Craniofac Surg. 2011; 22(4):1294-8.
[11] Bocskai Z, Bojtár I. Biomechanical modelling of the accommodation problem of human eye. Period Polytech Civ Eng. 2013; 57(1):3-9.
[12] Crouch JR, Merriam JC, Crouch ER. Finite element model of cornea deformation. Conf Proc Med Image Comput Comput Assist Interv. 2005; 8(2):591-8.
[13] Kling S, Marcos S. Finite-Element Modeling of Intrastromal Ring Segment Implantation into a Hyperelastic Cornea. Invest Ophthalmol Vis Sci. 2013; 54(1):881-9.
[14] Nejad TM, Foster C, Gongal D. Finite element modelling of cornea mechanics: a review. Arq Bras Oftalmol. 2014; 77(1):60-5.
[15] Power ED, Stitzel JD, West RL, Herring IP, Duma SM. A non linear finite elemente model of the human eye for large deformation loading. Conf Proc Biomech. 2001; 1:44-2.
[16] Rossi T, Boccassini B, Esposito L, Clemente C, Iossa M, Placentino L, Bonora N. Primary Blast Injury to the Eye and Orbit: Finite Element Modeling. Invest Ophthalmol Vis Sci. 2012; 53(13):8057-66.
[17] Sródka, W. Evaluating the material parameters of the human cornea in a numerical model. Acta Bioeng Biomech. 2011; 13(3):77-85.
[18] Studer H, Larrea X, Riedwyl H, Büechler P. Biomechanical model of human cornea based on stromal microstructure. J Biomech. 2010; 43(5):836-42.
[19] Uchio E, Ohno S, Kudoh J, Aoki K, Kisielewicz LT. Simulation model of an eyeball based on finite element analysis on a supercomputer. Br J Ophthalmol. 1999; 83(10):1106-11.
[20] Plagwitz KU. Studies on a new non-contact method of intraocular pressure measuring under considerations of the influence of the cornea thickness PhD thesis. Technische Universität Ilmenau; 2005.
[21] Remington LA. Clinical anatomy of the visual system. 2nd ed. Elsevier; 2005.
[22] Friberg TR, Lace JW. A comparison of the elastic properties of human choroid and sclera. Exp Eye Res. 1988; 47(3):429-36.
[23] Bisplinghoff JA, McNally C, Manoogian SJ, Duma SM. Dynamic material properties of the human sclera. J Biomech. 2009; 42(10):1493-7.
[24] Pollack IP, Viernstein LJ, Radius RL. An instrument for constant-pressure tomography. Exp Eye Res. 1979; 29(6):579-85.
[25] Wangsupadilok B, Horatanaruang O. The impact of central corneal thickness on intraocular pressure measured by non-contact tonometry. J Med Assoc Thai. 2011; 94(5):574-8.
[26] Weinreb RN, Brandt JD, Garway-Heath D, Medeiros F. Intraocular Pressure. 1st ed. Kugler Publications; 2007.
[27] Shaarawy T. Glaucoma: Medical diagnosis and therapy. 1st ed. Saunders/Elsevier; 2009.
[28] Boote C, Hayes S, Abahussin M, Meek KM. Mapping collagen organization in the human cornea: left and right eyes are structurally distinct. Invest Ophthalmol Vis Sci. 2006; 47(3): 901-8.
[29] Elsheikh A. Finite element modeling of corneal biomechanical behavior. J Refract Surg. 2010; 26(4):289-300.